Solar Scintillation Effects on Telecommunication Links at Ka-Band and X-Band

Y. Feria, M. Belongie, and T. McPheeters
Communications Systems and Research Section

H. Tan
Communications Systems and Research Section
and
University of California, Irvine

Many deep-space missions encounter solar conjunction. Some missions, such as Solar Probe and Stardust, encounter solar conjunction during their main missions. The Sun–Earth–Probe (SEP) angle is used to describe the degree of conjunction. When the SEP angle is small, the solar plasma causes degradation in telecommunication link performance. In this article, we present a model that we developed to study the amplitude scintillation effects on telemetry signals at both 8.4 GHz (X-band) and 32 GHz (Ka-band). Both analytical and simulated results show that, at a low bit-error rate ($<10^{-5}$), X-band links suffer degradation of 8.2 dB for the Solar Probe mission at perihelion. Ka-band links, however, suffer only a few tenths of a dB. In addition to this 8-dB Ka-band advantage over X-band under scintillation conditions, there is also the 4- to 6-dB Ka-band advantage due to higher frequency.

I. Introduction

Solar scintillation effects can be significant for deep-space telecommunication links at small Sun–Earth–Probe (SEP) angles. Severe scintillation can make the telecommunication link unavailable. An example is the Galileo mission near superior solar conjunction, where the 2.3-GHz (S-band) downlink began to experience degradation from solar scintillation as early as 1 month prior to superior conjunction. In fact, tracking of the Galileo telemetry was not possible from about 5 days prior to superior conjunction, at an SEP angle of 2.9 deg, until 7 days after, at an SEP angle of 5.8 deg, when a 2-dB symbol SNR was attained.[1]

Although the Galileo mission could temporarily tolerate an unavailable telecommunication link during superior solar conjunction, other missions, such as Solar Probe and Stardust, cannot because their main missions occur at superior conjunction. For example, the primary telemetry of interest in the Solar Probe mission is at perihelion with a Sun–Probe distance of 4 solar radii and a corresponding 1.066-deg SEP angle. This telemetry must be transmitted by the spacecraft as soon as possible to avoid data loss due

[1] J. Taylor, "Dates for 1996 Conjunction BVR Signal Loss, Reacquisition," personal communication, Jet Propulsion Laboratory, Pasadena, California, July 23, 1996.

to potential spacecraft damage from the solar corona near perihelion. The telecommunication link is required to function reliably in potentially severe scintillation conditions.

Scintillation effects are known to be less severe at higher frequencies. Future missions will employ 8.4 GHz (X-band). Moreover, 32 GHz (Ka-band) currently is being evaluated for deep-space communications. It is necessary to understand the effect of solar scintillation on telecommunication link performance at X-band and Ka-band. The objective of this work is to develop a simulation model and associated analysis to determine telecommunication link performance in the solar scintillation environment. We will use as an example the Solar Probe mission near perihelion and compare X-band telecommunication link performance to that at Ka-band.

A Rician statistical model of the scintillation channel is used in this work. This model is described in Section II, where the scintillation index for the Solar Probe mission near perihelion was provided by J. Armstrong.[2] Simulation of the full waveform receiver is extremely time consuming and not practical at the low coded bit-error rates (BERs) of interest. A semianalytical approach described in Section III combines a simplified simulation approach using an ideal receiver model and corresponding analytical performance estimates. Section IV describes the simulation of a full waveform receiver using a Block V receiver model. These full simulation results provided a validation of the simplified simulation and/or analytical approach for estimating telecommunication link performance at low BERs. These results show that while the degradation for the Solar Probe at perihelion for a coded BER of 10^{-5} is more than 8 dB at X-band, it reduces to only a couple of tenths of a dB at Ka-band. Some concluding remarks are given in Section V.

II. Scintillation Model

Our study of the effects of solar scintillation on telecommunication downlink performance will use as an example the Solar Probe mission near perihelion. A statistical model of the scintillation effects on radio propagation is required for simulation studies and associated analysis. Statistical models describing the effects of a random scattering medium on radio propagation have been widely studied in the past. These models have a wide range of detail and have varying degrees of compatibility with observed experimental results. In our choice of a suitable statistical model, we will focus only on first-order primary effects. Moreover, we shall only consider models with parameters that can be estimated directly from the Solar Probe mission design parameters.

Different scintillation-fading statistical models arise, depending on the geometry of the radio propagation path through the random scattering medium. When the receiver is far away from the scattering medium, and the scattering is weak, it is reasonable to assume that the received electric field is the sum of a large number of statistically independent waves scattered from different regions within the medium. Application of the central limit theorem leads to a complex-valued received signal with independent Gaussian real and imaginary parts. When the real and imaginary random components also are identically distributed, we obtain the Rician fading model with Rician-distributed signal amplitude. On the other hand, when the receiver is located in the scattering medium itself, the situation is quite different. In this case, particularly if the scattering is weak and the scattering cone is small, the received electric field is the result of multiplicative effects. It can thus be assumed to be the product of the incident field times a number of independent random multiplicative terms. Hence, application of the central limit theorem to the logarithm of the electric field leads to a received signal with Gaussian-distributed log-amplitude and phase. These are the well-known log-normal fading statistics. Semianalytic approaches have been adopted for other situations, yielding various fading distributions. The Nakagami m-distribution has

[2] J. W. Armstrong, "Approximate Scintillation U-Parameter Versus Sun–Earth–Probe Angle for X-Band Link, $\eta = 90°$ Solar Probe Telecommunications Geometry" JPL Interoffice Memorandum to W. V. Moore (internal document), Jet Propulsion Laboratory, Pasadena, California, July 17, 1994.

been received favorably for modeling intensity fading. The Fremouw two-component model combines the Rician and log-normal models.

Our objective is to develop a model that is reasonable for the Solar Probe mission, with parameters that can be readily estimated. Moreover, both amplitude and phase scintillation effects must be modeled to evaluate coherent demodulation. Of the models mentioned above, the Nakagami m-distribution does not directly model phase scintillation, and the two-component model has too many parameters. This leaves the Rician and log-normal fading models, both of which are compatible to some degree with the experimental intensity-fading solar-scintillation results studied by Armstrong and Woo.[3] Since the geometry of the Solar Probe mission is closer to that of the Rician fading physical model, we shall adopt Rician fading statistics in our simulation studies.

The fading strength for Rician statistics depends on the carrier frequency and the geometry of the Sun, Earth, and probe, or the SEP angle. It can be described in terms of the U-parameter,[4] which is the first Born approximation to the ratio of the variance of the fading intensity to the square of the mean intensity. With an orbital plane perpendicular to the Sun–Earth line, a distance from the center of the Sun to the Probe between 4 and 20 solar radii, and a carrier frequency at X-band (8.4 GHz), the U-parameter can be approximated as follows:[5]

$$U_X = 4.97\left(\frac{R}{R_0}\right)^{-3.05} + 252\left(\frac{R}{R_0}\right)^{-6} \quad \text{for } 4R_0 \le R \le 20R_0 \tag{1}$$

where R_0 is the radius of the Sun and R is the distance from the center of the Sun to the probe. The ratio R/R_0 is proportional to the SEP angle for small R. For the same geometry, but at Ka-band, the U-parameters in Eq. (1) for X-band can be scaled to Ka-band using the property that U varies inversely[6] with (frequency ratio)$^{2.6}$. That is,

$$U_{Ka} = \left(\frac{f_{Ka}}{f_X}\right)^{-2.6} U_X \tag{2}$$

where U_X is defined in Eq. (1). As noted by Armstrong,[7] the calculation of the U-parameter using Eq. (1) is for nominal scintillation conditions only. Transient solar events in particular can cause much worse scintillation than this calculation would indicate. The Rician fading distribution will be specified below in terms of the scintillation index m, which is the ratio of the standard deviation of the received signal intensity to its mean. It is related to the first Born approximation, U, by

$$m = \begin{cases} U^{1/2} & 0 \le U \le 1 \\ 1 & U > 1 \end{cases} \tag{3}$$

After propagating through a Rician fading channel, the received residual carrier signal at DSN ground stations can be written as

$$r(t) = \sqrt{2P}V \sin\left[\omega_c t + \phi_c + \phi_d(t) + \phi_R\right] + n(t) \tag{4}$$

[3] J. Armstrong and R. Woo, personal communication, Jet Propulsion Laboratory, Pasadena, California, July 1996.

[4] J. W. Armstrong, op cit.

[5] Ibid.

[6] Ibid.

[7] Ibid.

where P is the total received signal power; V is the Rician-distributed fading amplitude due to scintillation; ω_c and ϕ_c are the carrier angular frequency and phase, respectively; ϕ_R is the phase scintillation associated with Rician fading; and $n(t)$ is an additive white Gaussian noise accounting for receiver thermal noise as well as background noise. The data modulating signal, $\phi_d(t)$, is assumed to use a square-wave subcarrier and is given by

$$\phi_d(t) = \Delta d(t) \text{ sgn } [\sin(\omega_{sc}t + \phi_{sc})]$$

where Δ is the modulation index, $d(t) = \pm 1$ is the data, and ω_{sc} and ϕ_{sc} are the subcarrier angular frequency and phase, respectively.

Assume that the amplitude scintillation causes no loss in the long-term average received signal power. Then the Rician random variable V has second moment $\mathrm{E}[V^2] = 1$ and probability density function $p_V(\nu)$ given by

$$p_V(\nu) = \frac{\nu}{\sigma^2} \exp\left(-\frac{\nu^2 - a^2}{2\sigma^2}\right) \mathrm{I}_0\left(\frac{\nu a}{\sigma^2}\right), \quad \nu \geq 0 \tag{5}$$

In Eq. (5), a^2 is the deterministic signal power in V and σ^2 is the signal variance, for each part—real and imaginary. After normalization to satisfy the constraint of no long-term power loss ($2\sigma^2 + a^2 = 1$), it can be shown that the parameters a^2 and σ^2 are related to the scintillation index m by

$$a^2 = (1 - m^2)^{1/2} \tag{6}$$

and

$$\sigma^2 = \frac{1 - \sqrt{1 - m^2}}{2} \tag{7}$$

Expanding Eq. (4), we have

$$r(t) = \sqrt{2P}\,[V\cos(\phi_R)\sin(\omega_c t + \phi_c + \phi_d(t)) + V\sin(\phi_R)\cos(\omega_c t + \phi_c + \phi_d(t))] + n(t) \tag{8}$$

Define $X = V\cos(\phi_R)$ and $Y = V\sin(\phi_R)$. Then X and Y are independent Gaussian random variables with the same variance σ^2 because ϕ_R is independent of V and ϕ_R is in $[-\pi, \pi]$. Moreover,

$$E\{X\} = a = (1 - m^2)^{1/4}$$

$$E\{Y\} = 0$$

Finally, expanding the sine and cosine terms in Eq. (8) to explicitly separate the carrier component from the data modulation component, we can write

$$r(t) = \sqrt{2P}\cos\Delta\,[X\sin(\omega_c t + \phi_c) + Y\cos(\omega_c t + \phi_c)]$$

$$+ \sqrt{2P}\sin\Delta\, d(t)\text{sgn}\,[\sin(\omega_{sc}t + \phi_{sc})]\,[X\cos(\omega_c t + \phi_c) - Y\sin(\omega_c t + \phi_c)] + n(t) \tag{9}$$

Equation (9) is used as our simulation model for the received signal. The above Rician fading model does not specify the fade durations. Woo and Armstrong have studied the spectral characteristics of solar-scintillation amplitude fading. They have reported that the fading spectrum, which depends on carrier frequency, has a 3-dB autocorrelation time-lag width varying from 13.9 ms at S-band to 7.25 ms at X-band to 3.72 ms at Ka-band.[8] These are the fading durations assumed for our model at X-band and at Ka-band. Additive white Gaussian noise samples in Eq. (9) are generated independently for each sample in the simulations, but only one X and Y fading variable will be generated independently for each fade duration interval.

In the next section, we analytically determine the convolutionally encoded communication performance degradation, assuming that the fade duration is longer than the memory length of the Viterbi decoder and that perfect carrier and subcarrier tracking as well as symbol synchronization are achieved. The analysis is used to validate a simplified simulation model. Simulations also are presented at different fading durations where the analytical model is not valid.

III. Scintillation Effects for an Ideal Receiver

Simulation of the full waveform receiver is extremely time consuming and not practical at the low BERs of interest. Our approach to this problem is semianalytic in nature, where analysis and simulations are combined with the assumption of an ideal receiver, that is, the assumption of perfect carrier and subcarrier phase recovery and perfect symbol synchronization at the receiver as well as ideal integrate-and-dump demodulation for convolutionally coded communications. This speeds up the simulations by removing the signal waveform modulators and demodulators as well as the carrier, subcarrier, and symbol tracking loops. This simplified simulation approach is based on the link model, assuming an ideal receiver as shown in Fig. 1. An analytic model can be used to generate theoretical BER estimates to validate the simplified simulation approach when the fading durations are longer than the Viterbi decoder memory length. The analytic model also is useful for providing estimates of the performance degradation due to scintillation at low BERs, where simulation takes too long. Simulation of the complete waveform receiver is then performed at high BERs to calibrate the simplified simulation and analytic performance estimates. This semianalytic approach then can generate meaningful performance studies at low BERs, where simulation by itself is not practical.

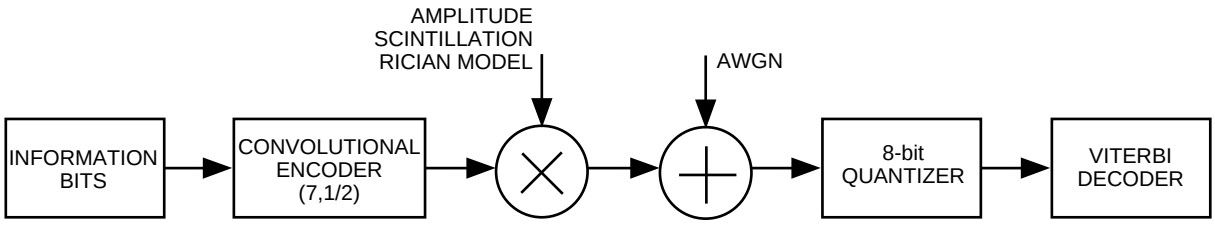

Fig. 1. A simplified block diagram of the telecommunication link bypassing the modulator and demodulator.

The simulation studies focused on the Solar Probe mission near perihelion where the Sun–Probe distance will be 4 solar radii with a 1.066-deg SEP angle. The simplified simulation effectively ignores the phase scintillation since perfect carrier tracking is assumed, so only amplitude scintillation is present. Amplitude scintillation is considered for a solar bypass trajectory at a 90-deg inclination to the ecliptic passing from the northern pole to the southern pole with a 4-solar radii perihelion encounter. A comparison of the communication performance degradation relative to a channel with no scintillation effects is made at both X-band and Ka-band.

[8] J. W. Armstrong and R. Woo, "Temporal Autocorrelation Functions and Fluctuation Power Spectra of Amplitude Scintillations: Starprobe–Earth Communication Geometry," JPL Interoffice Memorandum 3333-81-048 (internal document), Jet Propulsion Laboratory, Pasadena, California, May 29, 1981.

In this study, we used only the (7,1/2) convolutional code with Viterbi decoding, which is the code that the Solar Probe mission plans to use. However, this methodology can easily be extended in the future to include other coding schemes for comparison.

A. Analytical Model

In this analysis, the degradation caused by amplitude scintillation is determined for the case of a (7,1/2) convolutional code and coherent binary phase shift keying (BPSK). The analytical model assumes that each fade duration is sufficiently long to cover the memory length of the Viterbi decoder for a (7,1/2) convolutional code. Assuming no scintillation effects, perfect carrier and subcarrier tracking, perfect symbol synchronization, and an ideal matched-filter demodulator, the BER performance of a (7,1/2) convolutionally encoded, 8-bit quantized Viterbi decoded link can be written as

$$P_b = f\left(\frac{E_b}{N_0}\right) \tag{10}$$

where a good approximation of the function, $f(x)$ (generated by curve fitting the simulation points from a software Viterbi decoder), is given by

$$f(x) = \begin{cases} 0.5 & 0 \le x \le 0.40096515 \\ 0.526982 + 0.138613x - 0.513525x^2 & 0.40096515 < x < 1.047 \\ \exp(-6.2440662x + 4.6399841) & x > 1.047 \end{cases}$$

A curve for this function is shown in Fig. 2, labeled as "no scintillation."

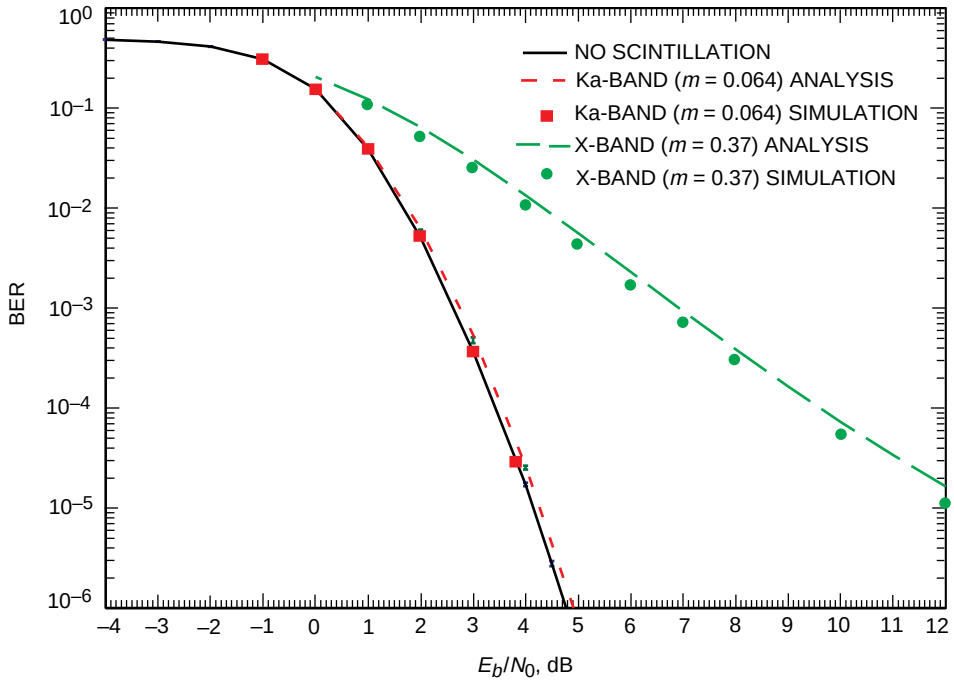

Fig. 2. Telecommunication link performance under scintillation effects: Ka-band versus S-band ($R = 4R_o$ and fade duration = 200 bits).

Assume that the data transmission rate is much larger than the inverse of the fade duration, so that the received RF signal amplitude is constant over the Viterbi decoder memory length. Then the corresponding (7,1/2) convolutionally encoded bit-error probability in this scintillation environment is obtained by a statistical average of the static performance in Eq. (10) over the Rician amplitude scintillations:

$$P_b = \int_0^\infty f\left(\nu^2 \frac{E_b}{N_0}\right) p_V(\nu) d\nu \tag{11}$$

For a given SEP angle, the U-parameters at X-band, obtained from Eq. (1) and scaled to Ka-band using Eq. (2), determine the scintillation index m shown in Eq. (3). This scintillation index is used in Eqs. (6) and (7) to determine the mean and variance of the Rician density shown in Eq. (5). This Rician density then is used in Eq. (11) to obtain the coded bit-error probability performance in the environment where receiver synchronization is perfect and only amplitude scintillation is present. Comparison to the coded bit-error probability performance given by Eq. (10) in the absence of scintillation effects then yields the degradation in E_b/N_0 caused by amplitude scintillation alone in this idealized situation when the fade durations are sufficiently long (see results in Fig. 2).

B. Simulation Results

A comparison will be made first between the analytical model described above and the simulation results obtained through the simplified simulation approach. In the first comparison, the fade duration is assumed to be longer than the memory length of the Viterbi decoder for the (7,1/2) convolutional code. We use a fade duration of 200 channel symbols. This is substantially longer than the decoder memory length (truncation length), which is 64 bits (128 channel symbols) for the DSN's (7,1/2) convolutional decoder. Figure 2 displays the link BER performance results as a function of E_b/N_0 at both X-band and Ka-band, where the probe is assumed to be at perihelion with a 4-solar radii distance to the center of the Sun. Here the analytical results are virtually identical to the simulations at Ka-band, and they are within a few tenths of a dB at X-band. The analytical results generally are slightly more pessimistic than the simulations, with the deviations increasing at a lower BER for X-band. The much larger scintillation index at X-band ($m = 0.37$) than at Ka-band ($m = 0.064$) results in a much higher performance degradation. Both the simulations and analytical results show that at BER=10^{-5}, which is the usual requirement for deep-space telecommunication links, the link performance at X-band degrades more than 8 dB, while the Ka-band performance degrades less than 0.2 dB. These results indicate a good agreement between the simulations and the analytical results.

Figure 3 displays the link BER performance as a function of E_b/N_0 at X-band only, where the probe-to-Sun-center distance is varied from 4 to 8 solar radii. The scintillation index decreases from $m = 0.37$ at 4 solar radii to $m = 0.099$ at 8 solar radii, reducing the link degradation from over 8 dB to about 0.4 dB at $BER = 10^{-5}$. Here a good agreement between the simulations and the analytical results again is obtained.

These results confirm the agreement between the analytical and simplified simulation models. However, as we shall see, this agreement depends crucially on the fade duration being sufficiently longer than the decoder memory length. Figure 4 displays the link BER performance as a function of E_b/N_0 at X-band only, with a 4-solar radii probe-to-Sun-center distance when the fade duration is varied. Here fade durations are taken to be 1000, 200, 50, and 10 channel symbols. The simulations are virtually identical to the analytical results at a 1000-symbol fade duration and have a deviation of at most a few tenths of a dB at a 200-symbol fade duration. However, the deviations increase substantially as the fade durations are decreased to 50 symbols and 10 symbols. The analytical model breaks down when the fade duration is shorter than the Viterbi decoder memory length. Since the decoder memory length is 64 bits, or 128 channel symbols, for the DSN's (7,1/2) decoder, the increasing deviations between the simulations and analytical results at shorter fade durations are not surprising. For short fade durations where the

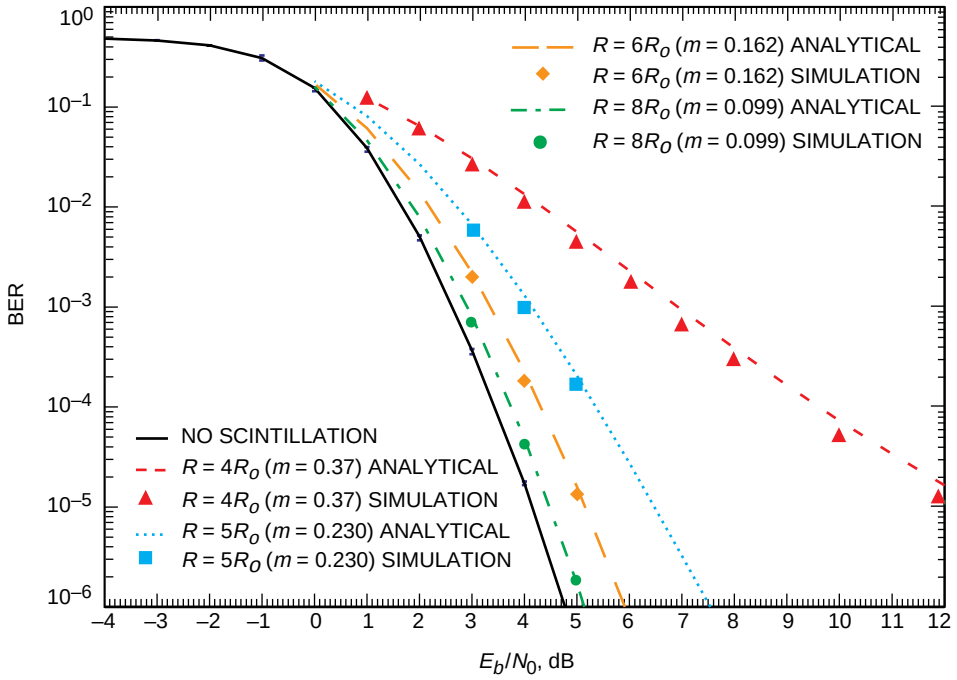

Fig. 3. Telecommunication link performance at X-band: a comparison at different distances from the center of the Sun (fade duration = 200 bits).

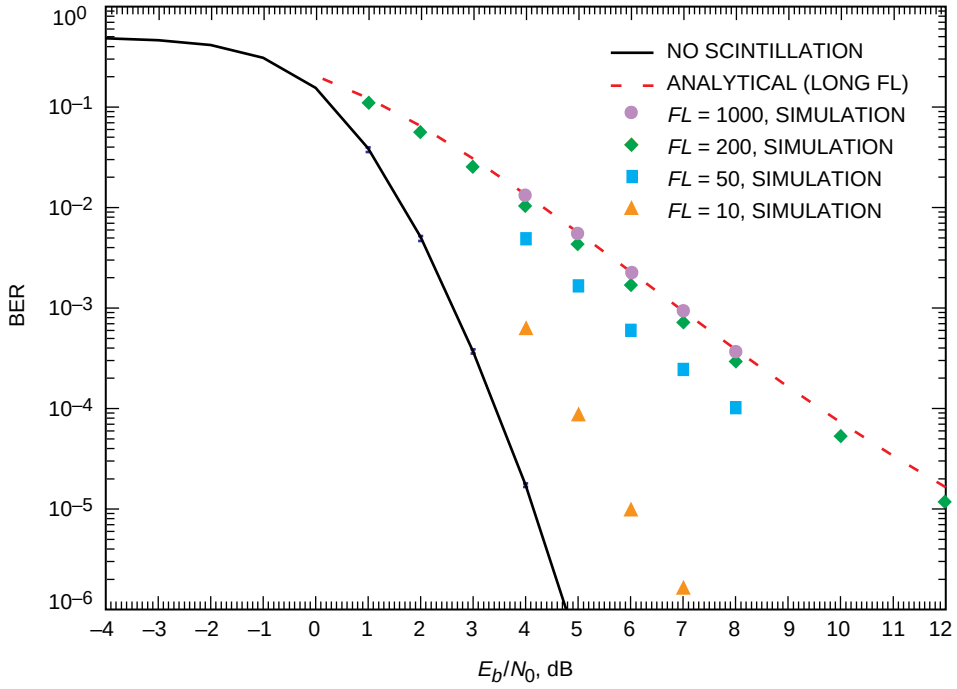

Fig. 4. Telecommunication link performance at X-band at 4 solar radii with different fade lengths (FLs).

analytical model is not valid, simulations are more reliable. Note that the analytical model in Eq. (11) is pessimistic, because it does not account for the decoder being able to average over several fades occurring in its path memory.

Recall that the solar-scintillation fading spectrum has a 3-dB autocorrelation time-lag width of 7.25 ms at X-band and 3.72 ms at Ka-band.[9] Depending on the data rate, a fade duration can be a few bits to a few hundred bits long. Assuming a data rate of 4 kbits/s, a 7.25-ms fade duration covers 58 channel symbols at X-band. The corresponding 3.72-ms fade duration at Ka-band covers 30 channel symbols.

IV. Scintillation Effects Using the Block V Receiver

Simulation of the complete waveform receiver was performed to calibrate the simplified simulation and analytic results described in the last section. The link simulator for this task consisted of a (7,1/2) convolutional encoder, a modulator, the Rician amplitude and phase fading statistics, plus an additive white Gaussian noise channel, a software Block V receiver, and a Viterbi decoder with 8-bit quantization as shown in Fig. 5. These time-consuming simulations could only be performed at high BERs. A fade duration of 200 symbols was used for all the simulations, so the analytic model of the last section is valid for the corresponding simplified simulations considering amplitude scintillation only.

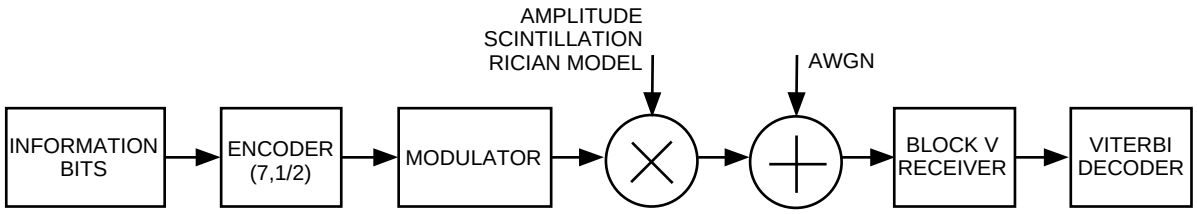

Fig. 5. The link simulation model using the Block V receiver.

The first simulations were performed for both X-band and Ka-band when the probe-to-Sun-center distance is equal to 4 solar radii. Measurements were taken of the BER at the decoder output, the SER at the receiver output, the symbol SNR at the receiver output, the carrier and subcarrier loop lock indicators, and the carrier and subcarrier phase jitters. Both the carrier and subcarrier loops were able to track without losing lock in the presence of Rician phase scintillation. Figure 6 plots the simulated coded BER performance results versus E_b/N_0 along with the analytical performance estimates of the last section. There appears to be good agreement between the full simulation results and the analytic performance estimates at both X-band and Ka-band. The deviation of the simulated X-band performance from the analytical result at BER = 0.002 is probably due to statistical error, since a sufficiently long simulation run could not be accomplished in this study for this BER.

In a second set of simulations, we fixed $E_b/N_0 = 2.3$ dB and varied the scintillation index. Figure 7 plots the simulated decoder BER results as a function of the scintillation index m along with the corresponding analytic performance estimates of the last section. Again, good agreement between the simulation results and the analytical performance estimates was obtained. These sets of full simulation results indicate that the simplified simulation approach and/or the analytical model can be reliably used to estimate telecommunication link performance in a scintillation environment with Rician statistics and long fade durations.

[9] Ibid.

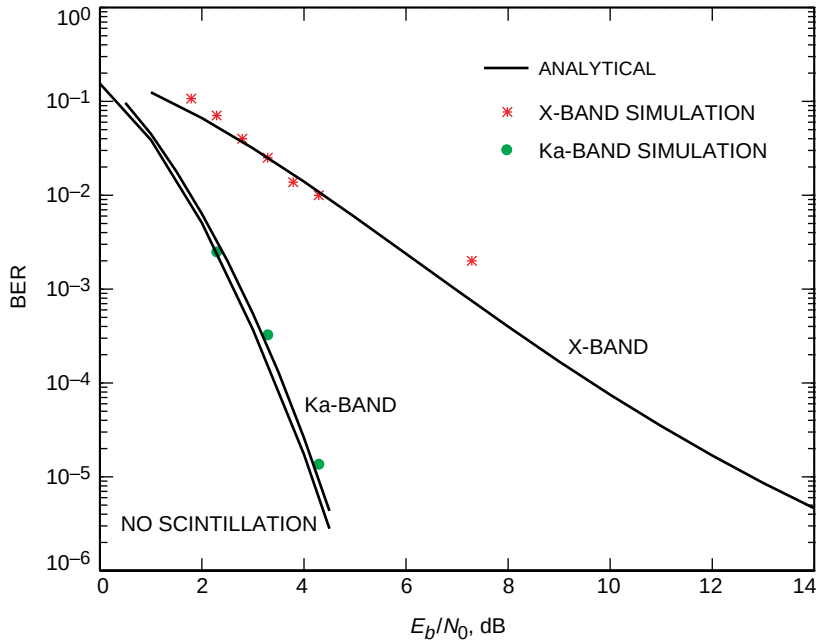

Fig. 6. Block V receiver performance at 4 solar radii at X-band and Ka-band (fade duration = 200 symbols).

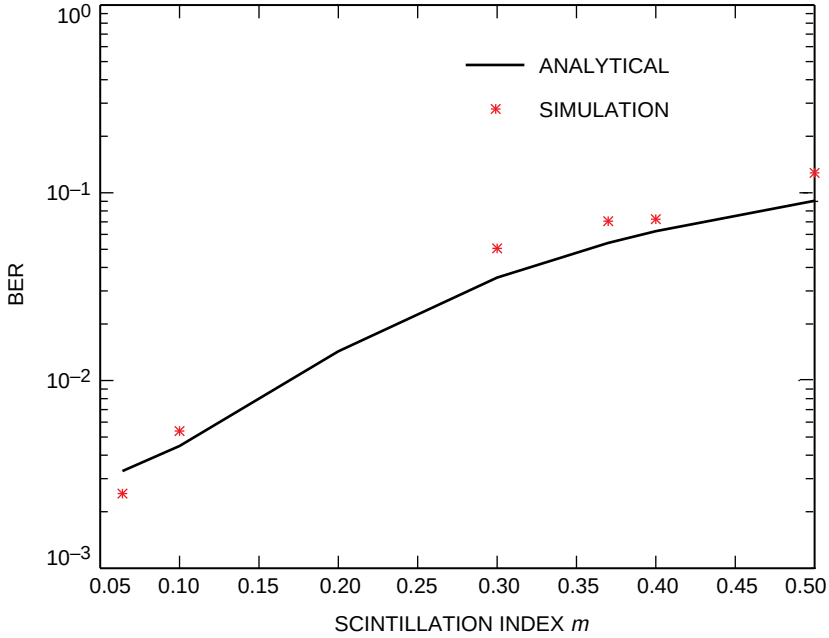

Fig. 7. Block V receiver performance at E_b/N_0 = 2.3 dB and different scintillation indices (fade duration = 200 symbols).

V. Conclusion and Future Work

This study used a Rician statistical model of the solar scintillation channel. It was shown that while communication link performance at Ka-band will suffer a negligible degradation under nominal conditions, large performance degradation likely will occur at X-band. The carrier, subcarrier, and symbol synchronization tracking loops did not seem to be affected by the solar scintillation.

Previous measured solar scintillation data indicate that the Rician model is not accurate when the scintillation index is close to one. An analysis of existing scintillation data should be performed to identify other statistical models of both amplitude and phase scintillation effects on the received modulation signal. Such models would be useful for generating more accurate simulation and analytical comparisons between X-band and Ka-band communications capabilities. We also would like to expand the study to include different coding schemes, such as concatenated Reed–Solomon and convolutional (7,1/2) code and turbo codes. The appropriate code block length for a given fading duration can be studied.

Acknowledgments

The authors wish to thank John Armstrong, Sam Dolinar, Bill Moore, Jim Randolph, and Richard Woo for their valuable suggestions and discussions.